Interpretation of Approximate Entropy: Analysis of Intracranial Pressure Approximate Entropy During Acute Intracranial Hypertension

Roberto Hornero, *Member, IEEE*, Mateo Aboy, *Member, IEEE*, Daniel Abásolo, *Member, IEEE*, James McNames, *Senior Member, IEEE*, and Brahm Goldstein, *Associate Member, IEEE*

***Abstract*—We studied changes in intracranial pressure (ICP) complexity, estimated by the approximate entropy (ApEn) of the ICP signal, as subjects progressed from a state of normal ICP (< 20–$25\ \mathrm{mmHg}$) to acutely elevated ICP (an ICP "spike" defined as ICP $> 25\ \mathrm{mmHg}$ for $\leq 5\ \mathrm{min}$). We hypothesized that the measures of intracranial pressure (ICP) complexity and irregularity would decrease during acute elevations in ICP. To test this hypothesis we studied ICP spikes in pediatric subjects with severe traumatic brain injury (TBI). We conclude that decreased complexity of ICP coincides with episodes of intracranial hypertension (ICH) in TBI. This suggests that the complex regulatory mechanisms that govern intracranial pressure are disrupted during acute rises in ICP. Furthermore, we carried out a series of experiments where ApEn was used to analyze synthetic signals of different characteristics with the objective of gaining a better understanding of ApEn itself, especially its interpretation in biomedical signal analysis.**

***Index Terms*—Approximate entropy, complex analysis, intracranial hypertension, intracranial pressure irregularity, sample entropy, traumatic brain injury (TBI).**

I. Introduction

SERIES of sequential data occur throughout epidemiology in multiple contexts. Enhanced capabilities to quantify differences among such series would be extremely valuable, since these time series reflect essential biological processes. Although practitioners and researchers typically quantify mean levels, and often the extent of variability, it is recognized that in many instances, the persistence of certain patterns in biologic signals provide fundamental insight [1].

The historical development of mathematics to quantify regularity has centered on various types of entropy measures. Entropy is a measure of randomness and predictability of a stochastic process. It generally increases with greater randomness. Kolmogorov–Sinai (K-S) entropy, developed by Kolmogorov and expanded upon by Sinai, allows classification of deterministic dynamical systems by rate of information generation [2]. Unfortunately, K-S entropy was not developed for statistical applications, and its blind application to practical time series will only evaluate system noise, not underlying system properties, as it generally requires a vast amount of input data to achieve convergence [3].

Approximate entropy (ApEn) is a family of parameters and statistics recently introduced to quantify regularity in data without any *a priori* knowledge about the system generating them [4]. It was constructed by Pincus, motivated by applications to short and noisy data sets, along thematically similar lines to K-S entropy [5]. However, the focus was, in this case, to provide a widely applicable, statistically valid formula that will distinguish data sets by a measure of regularity [5]. The observation motivating ApEn is that if joint probability measures of reconstructed dynamics that describe each of two systems are different, then their marginal probability distributions on a fixed partition, given by conditional probabilities, are likely different. Typically, orders of magnitude fewer points are needed to accurately estimate these marginal probabilities than to accurately reconstruct the attractor measure defining the process [1].

Based on numerous studies, ApEn may correlate with "hidden" or subclinical changes often undetected by other more classical time series analysis, including both moment statistics, spectral analysis, and correlation analysis. ApEn changes have often been seen to be predictive of subsequent clinical changes. This has facilitated the application of ApEn to numerous settings both within and outside biology. Within biology and medicine, it has been applied to studies discriminating atypical EEG's [6] and respiratory patterns [7] from normative counterparts. Furthermore, it has been used to quantify the differences in apparent regularity between the heart rate interval time series of aborted SIDS and healthy infants [8] and to characterize postoperative ventricular dysfunction [9]. Preliminary evidence suggests that ApEn of EEG's is predictive of epileptic seizures [10]. It has also been applied to extract features from EEG and respiratory recordings of a patient during Cheyne-Stokes respiration [11] and to quantify the depth of anesthesia [12]. Within endocrinology, it has been used in multifaceted ways; for instance, in the analysis of endocrine hormone release pulsatility [13], and the impact of pulsatility on the ensemble orderliness of neurohormone secretion [14].

Manuscript received June 7, 2004; revised November 28, 2004. This work was supported in part by the Thrasher Research Fund, in part by the Northwest Health Foundation, in part by the Doernbecher Children's Hospital Foundation, and in part by the grant project of Junta de Castilla y León no. VA019-04. *Asterisk indicates corresponding author.*

R. Hornero and D. Abásolo are with the Department of Signal Theory and Communications, ETSIT, University of Valladolid 47011, Valladolid, Spain.

*M. Aboy is with the Electronics Engineering Technology Department, Oregon Institute of Technology, Portland, OR 97229 USA and also with the Biomedical Signal Processing Laboratory, Department of Electrical and Computer Engineering at Portland State University, 1900 SW 4th Ave., Portland, OR 97201 USA (e-mail: mateoaboy@ieee.org).

J. McNames is with the Biomedical Signal Processing Laboratory, Department of Electrical and Computer Engineering at Portland State University, Portland, OR 97201 USA.

B. Goldstein is with the Complex Systems Laboratory in the Department of Pediatrics, Oregon Health and Science University, Portland, OR 97201 USA.

Digital Object Identifier 10.1109/TBME.2005.855722

The capability of ApEn to assess subtle disruptions, typically preceding changes in signal mean and variance, holds the potential for enhanced preventive and earlier interventionist strategies [1].

In this paper, we applied the concept of ApEn to intracranial pressure signals (ICP) obtained from patients with traumatic brain injury (TBI) during periods of acute elevations in intracranial pressure, so-called "ICP spikes." TBI is the leading cause of death and disability in children in the United States [15]. Elevated ICP following TBI often results in secondary injury due to decreased cerebral perfusion pressure[1] (CPP) and cerebral ischemia[2]. ICP monitoring and therapeutic interventions to control elevated ICP (> 20 mmHg) have resulted in improved outcomes [16]–[18].

We estimated the ApEn during ICP spikes. Additionally, we carried out a series of experiments using synthetic signals with the objective of getting a better understanding of ApEn itself, and how to interpret it in the context of biomedical signal analysis.

The simulation study was designed to find the relationship between the ApEn metric and classical signal processing concepts such as frequency, number of harmonics, frequency variability of harmonics, and signal bandwidth.

II. Methods: ApEn

ApEn was introduced as a quantification of regularity in sequences and time series data, initially motivated by applications to relatively short, noisy data sets. Mathematically it is part of a general development of approximating Markov Chains to a process [19]. It provides a finite sequence formulation of randomness, via proximity to maximal irregularity [20]. A statistical evaluation of ApEn is available in [4]. ApEn is scale invariant and model independent, evaluates both dominant and subordinant patterns in data, and discriminates series for which clear feature recognition is difficult. Notably it detects changes in underlying episodic behavior not reflected in peak occurrences or amplitudes [21]. It is applicable to systems with at least 50 data points and to broad classes of models; it can be applied to discriminate both general classes of correlated stochastic processes, as well as noisy deterministic systems. Moreover, ApEn is complementary to spectral and autocorrelation analyzes, providing effective discriminatory capability in instances in which the aforementioned measures exhibit minimal distinctions [1]. It is nearly unaffected by low level noise, is also robust to meaningful information with a reasonable number of data points, and is finite for both stochastic and deterministic processes [12]. It measures the logarithmic likelihood that runs of patterns that are close remain close on subsequent incremental comparisons, and assigns a nonnegative number to a time series, with larger values corresponding to more complexity or irregularity in the data. ApEn has two user-specified parameters: a run length m and a tolerance window r. It is important to consider $\mathrm{ApEn}(m, r)$—or $\mathrm{ApEn}(m, r, N)$, where N is the number of points of the time series—as a family of parameters: comparisons between time series segments can only be made with the same values of m and r[1]. Formally, given N data points from a time series $\langle x(n)\rangle = \{x(1), x(2), \ldots, x(N)\}$, the ApEn is computed as follows.

1) From m-vectors $X(1), X(2), \ldots, X(N-m+1)$ defined as $X(i) = [x(i), x(i+1), \ldots, x(i+m-1)]$, $i = 1, 2, \ldots, N-m+1$. These vectors represent m consecutive x values, commencing with the ith point.
2) Calculate the distance between $X(i)$ and $X(j)$, $d[X(i), X(j)]$, as the maximum absolute difference between their respective scalar components

$$d[X(i), X(j)] = \max_{k=1,2,\ldots,m} (|x(i+k-1) - x(j+k-1)|). \quad (1)$$

3) For a given $X(i)$, count the number of j ($j = 1, 2, \ldots, N-m+1$) for $j \neq i$ such that $d = [X(i), X(j)] \leq r$, denoted as $N^m(i)$. Then, for $i = 1, 2, \ldots, N-m+1$

$$C_r^m(i) = \frac{N^m(i)}{N-m+1}. \quad (2)$$

The $C_r^m(i)$ values measure, within a tolerance r, the regularity (frequency) of patterns similar to a given one of window length m.
4) Compute the natural logarithm of each $C_r^m(i)$, and compute the average of it over i

$$\phi^m(r) = \frac{1}{N-m+1} \sum_{i=1}^{N-m+1} \ln C_r^m(i) \quad (3)$$

where $\phi^m(r)$ represents the average frequency of all the m-point patterns in the sequence remain close to each other.
5) Increase the dimension to $m+1$. Repeat steps 1) to 4) and find C_r^{m+1} and $\phi^{m+1}(r)$.
6) Theoretically, the ApEn is defined as

$$\mathrm{ApEn}(m, r) = \lim_{N \to \infty} \left[\phi^m(r) - \phi^{m+1}(r)\right]. \quad (4)$$

There are two ways to look at ApEn. From one point of view, it is a statistical metric (the average of the logarithm of a conditional probability), which makes it applicable to both deterministic and stochastic processes. From another point of view, it reflects the rate of new pattern generation and is thus related to the concept of entropy [22].

In practice, the number of data points N is finite. We implemented this formula by defining the statistic [5]

$$\mathrm{ApEn}(m, r) = \phi^m(r) - \phi^{m+1}(r). \quad (5)$$

Although m and r are critical in determining the outcome of ApEn, no guidelines exist for optimizing their values. In principle, the accuracy and confidence of the entropy estimate improve as the number of matches of length m and $m+1$ increases. The number of matches can be increased by choosing small m (short templates) and large r (wide tolerance). However, there are consequences for criteria that are too relaxed [5]. For smaller r values, one usually achieves poor conditional probability estimates, while for larger r values, too much detailed system information is lost. To avoid a significant contribution of noise in an ApEn calculation, one must choose r larger than most of the noise [1]. Furthermore, as m decreases,

[1]The CPP is defined as the difference between the systemic arterial blood pressure and the intracranial pressure, $\mathrm{CPP} = \mathrm{ABP} - \mathrm{ICP}$.

[2]Ischemia is a decrease in blood supply caused by constriction or obstruction of the blood vessels or decreased blood volume.

underlying physical processes that are not optimally apparent at smaller values of m may be obscured [23].

In this study, ApEn was estimated with the established parameter values of $m = 1$, $m = 2$ and $r = 0.1$, 0.15, 0.2, 0.25 times the standard deviation (SD) of the original data sequence. Normalizing r in this manner gives ApEn a translation and scale invariance, in that it remains unchanged under uniform process magnification, reduction, or constant shift to higher or lower values [1]. Several studies have demonstrated that these input parameters produce good statistical reproducibility for ApEn for time series of length $N = 60$, as considered herein [5], [21],[24].

III. Study Design

This study consisted of two parts. In the first part, we measured changes in the ICP complexity, estimated by the ApEn, as subjects progressed from a stable state of normal ICP (<20–25 mmHg) through an ICP spike (ICP > 25 mmHg). We hypothesized that the measures of ICP complexity such as the ApEn would decrease during the ICP spike and return toward pre-spike levels following resolution. To test this hypothesis we studied ICP spikes in pediatric patients with severe TBI.

The second part of the study consisted in performing a series of experiments where ApEn was used to analyze synthetic signals of different characteristics with the objective of gaining a better understanding of ApEn itself, specifically regarding its interpretability in the context of TBI.

A. ICP Database and Spike Detection

Data for this study was obtained from the physiological signal library of the Complex System Laboratory [25]. The database consist of 96 GB of ICP data collected from 93 patients from 1998–2003 who were admitted to the Pediatric Intensive Care Unit of the Doernbecher Children's Hospital (Oregon Health and Science University). ICP was monitored continuously using an intraventricular catheter or parenchymal fiber-optic pressure transducer (Integra NeuroCare, Integra LifeSciences, Plainsboro, NJ). The ICP monitor was connected to a Philips Merlin patient monitor (Philips, Best, Netherlands) that sampled the ICP and ABP signals at 125 Hz. An HPUX workstation automatically acquired these signals through a serial data network, and they were stored in files on CD-ROM. A detail description of the data acquisition can be found in [25].

We used the following criteria to define and detect ICP spikes.

1) The difference between the minimum value in the acutely elevated region of ICP and the maximum value in the stable ICP region must be at least 10 mmHg. This ensured that the detector only detected significant elevations of at least 10 mmHg that occur over a period of no more than 5 min.
2) The minimum value during the ICP spike must be greater than 20 mmHg. This ensured that each elevation was large enough to be clinically significant [17].
3) The mean ICP must be in the range of 0–100 mmHg in the stable region and less than 150 mmHg in the ICP spike. These criteria were used to limit artifact from being detected as spikes.

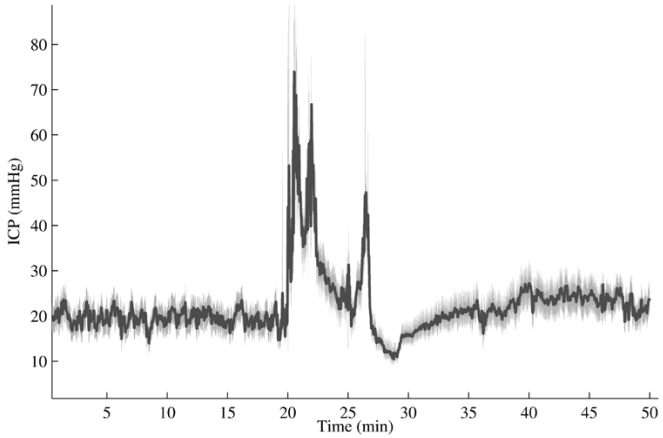

Fig. 1. Illustration of a typical ICP spike analyzed in this study. The light grey is the ICP signal waveform sampled at 125 Hz, and the dark line is the moving average ICP pressure. All ICP segments studied were 50 min long, with the onset of the ICH period synchronized at minute 20.

4) Each spike must be separated from preceding spikes by at least 5 min. This ensured that a single long elevation was not detected as two separate spikes.

Acute elevations in ICP that met the specified criteria were visually screened for artifact by consensus panel (ME and JM). This screen was based on a plot of the ICP signal spanning 20 min before the leading edge of the spike and 30 min after, as well as visualization of the spectrogram of the same segment. The visual screen eliminated candidate spikes if 1) they contained artifact, 2) there was an abrupt drop in the ICP signal consistent with cerebrospinal fluid (CSF) drainage, 3) the signal was clipped, or 4) the ICP spike was part of the same ICP elevation as the preceding spike. If the signal had none of these problems at any point in the 50-min record, the spike was included in this study.

In Fig. 1, we show an example of a typical ICP spike analyzed in this study.

B. Patients and Patient Management

The automatic spike detection algorithm above found 166 ICP segments that met our criteria for an acute spike. During the visual screen we found that 31 of the segments contained artifact, 28 of which were actually periods of cerebral spinal fluid drainage when the ventriculostomy catheter was turned off to the pressure monitor and created a *false* spike. An additional 95 segments were *clipped* at the maximum range of the patient monitor (i.e., the top or bottom of the ICP waveform was cut off creating signal artifact not suitable for analysis. One segment was identified as a second detection of a single hypertensive episode. The end result was 11 clean records of ICP spikes detected from 7 different subjects that were used for analysis

This study included 11 ICP spikes from 7 subjects with brain injury admitted to the pediatric ICU at Doernbecher Children's Hospital. The subjects age, gender, admission Glasgow Coma Scale score, and outcome are listed in Table I. Management of severe TBI followed the recently published "Guidelines for the Acute Medical Management of Severe Traumatic Brain Injury in Infants, Children, and Adolescents" [26].

The study protocol was reviewed and approved by the Institutional Review Board at Oregon Health & Science University. The requirement for informed consent was waived.

TABLE I
SUBJECT CHARACTERISTICS

Subject	Age	Gender	Brain Injury Description	GCS	Survival	GOS
1	9.5	F	Fall of horse. Depressed skull fracture, IPH, cerebral edema	7	Y	4
2	4.5	M	MVA. Skull fracture, SDH, cerebral edema	3	Y	3
3	8	M	S/P Craniosysostosis repair at age 2	15	Y	NA
4	4.75	F	MVA. Skull fracture, IPH, cerebral edema	5	Y	2
5	11.5	F	MVA. Skull fracture, SDH	8	Y	3
6	12.5	M	Gun Shot Would. IPH, SDH, cerebral edema	4	Y	4
7	15.8	M	Fall of skateboard. Depressed skull fracture, IPH, cerebral edema	3	Y	3

GCS = Glasgow Coma Score, GOS = Glasgow Outcome Score, IPH = Intraparenchymal hematoma, MVA = Motor Vehicle Accident, SDH = Subdural Hematoma

C. Statistical Analysis

Statistical analysis was aimed at determining the statistical significance of the mean reduction in ApEn during the ICH period for each of the individual subjects and across the population. Mean ApEn values were obtained for 2–min windows immediately before, during, and after the ICH period. We used bootstrap to estimate the standard error of the means for each of these states. We performed a nonparametric hypothesis test in order to determine statistically significant mean ApEn reductions based on bootstap. The main advantage of bootstrap technique is that is that it can be used to assess the statistical significance of these reductions without making any assumptions about the distribution of the mean ApEn reductions. The nonparametric bootstrap hypothesis testing involves computing a bootstrap confidence interval for the difference of mean ApEn. Equality of the mean ApEn is obtained if zero is a possible value in the CI. Results were considered to be statistically significant if $p < 0.01$.

D. Interpretability Tests and Synthetic Signals

Since our main objective for applying the ApEn metric to synthetic signals was to gain a better understating of what ApEn quantifies and to better interpret the results of our study with ICP signals during ICH in TBI, we limited the scope of our tests to signal parameters in the range of physiological interest.

1) ApEn Versus Frequency: The first test consisted in analyzing how changes in amplitude and frequency of sinusoidal signals affected the ApEn. For this purpose we generated two synthetic signals. The first of these consisted in a constant amplitude chirp signal whose frequency was swept linearly from 0.5 Hz to 5 Hz in 40 s. The second signal was created by modulating the amplitude of the chirp signal by a pure sinusoid. ApEn was applied to each of the two signals using a moving window of 10 s with 90% overlap with the objective of testing whether or not ApEn is sensitive to frequency or amplitude changes. Fig. 2(a) and (c) shows the constant chirp signal, the amplitude modulated chirp, and the spectrogram of the amplitude modulated chirp, respectively.

2) ApEn Versus Frequency Content: This test was designed to determine the relationship of ApEn and the frequency content of periodic signals. We generated four periodic signals of 10 s in duration with 1, 2, 5, and 7 frequency components, respectively. The four signals were concatenated and the ApEn metric was applied to the resulting vector using a moving window of 10 s with 90% overlap. Fig. 2(d) shows the composite signal used in this test.

3) ApEn Versus Sinusoid Plus Noise: The objective of this test was to determine if ApEn is sensitive to changes in noise power present in quasi-periodic signals. For this purpose we generated an amplitude-modulated sinusoid 40 s in duration, and added white Gaussian noise of various power to different portions of the signal. The noise power was increased every 10 sS (1, 1.1, 1.3 and 1.5). The ApEn metric was applied to the resulting vector using a moving window of 10 s with 90% overlap. Fig. 2(e) shows the sinusoid plus noise signal.

4) ApEn Versus Noise Power: In this test, the ApEn was applied using a moving window of 10 s with 90% overlap to a 40-swhite Gaussian noise sequence with power increasing in steps each 10 s (0.1, 0.3, 0.5 and 0.7). The objective of this test was to determine if given the same underlying signal structure (white noise) the ApEn is affected by the power of the noise. Fig. 2(f) shows this signal in the time domain.

5) ApEn Versus Noise Bandwidth: This test consisted of determining the the relationship between ApEn and the noise bandwidth. The synthetic signal consisted on a 40-stime series composed of 4 segments of colored noise with increasing spectral bandwidth. The ApEn metric was applied using a moving window of 10 s with 90% overlap. Fig. 2(g) and (h) show the signal in this time domain and its spectrogram, respectively.

6) ApEn Versus Simulated Icp Signals: The simplest model of pulsatile pressure consists of a pure sinusoid with a dc component

$$p(t) = \mu_p + P\cos(2\pi f_c t) \tag{6}$$

where μ_p corresponds to the mean pressure, P is the pulse amplitude, and f_c is the cardiac frequency. Thus, the previous simulation involving a pure sinusoid can be used to gain understanding of ApEn interpretability in the context of ICP

A more realistic model of ICP signals must take into account the pulse morphology, its variability, and the effects of respiration on the pressure signal. There is abundant literature on respiration and respiratory modulation of human autonomic rhythms [27]–[31]. There are three primary effects of respiration on pressure signals: pulse amplitude variation (AM), respiratory sinus arrythmia (frequency modulation), and an additive effect.

The AM accounts for part of the pulse pressure changes and we modeled as a double-sideband large carrier AM, also known as conventional AM

$$\phi_{AM}(t) = A_c[1 + am_n(t)] \cdot \cos 2\pi f_c t \tag{7}$$

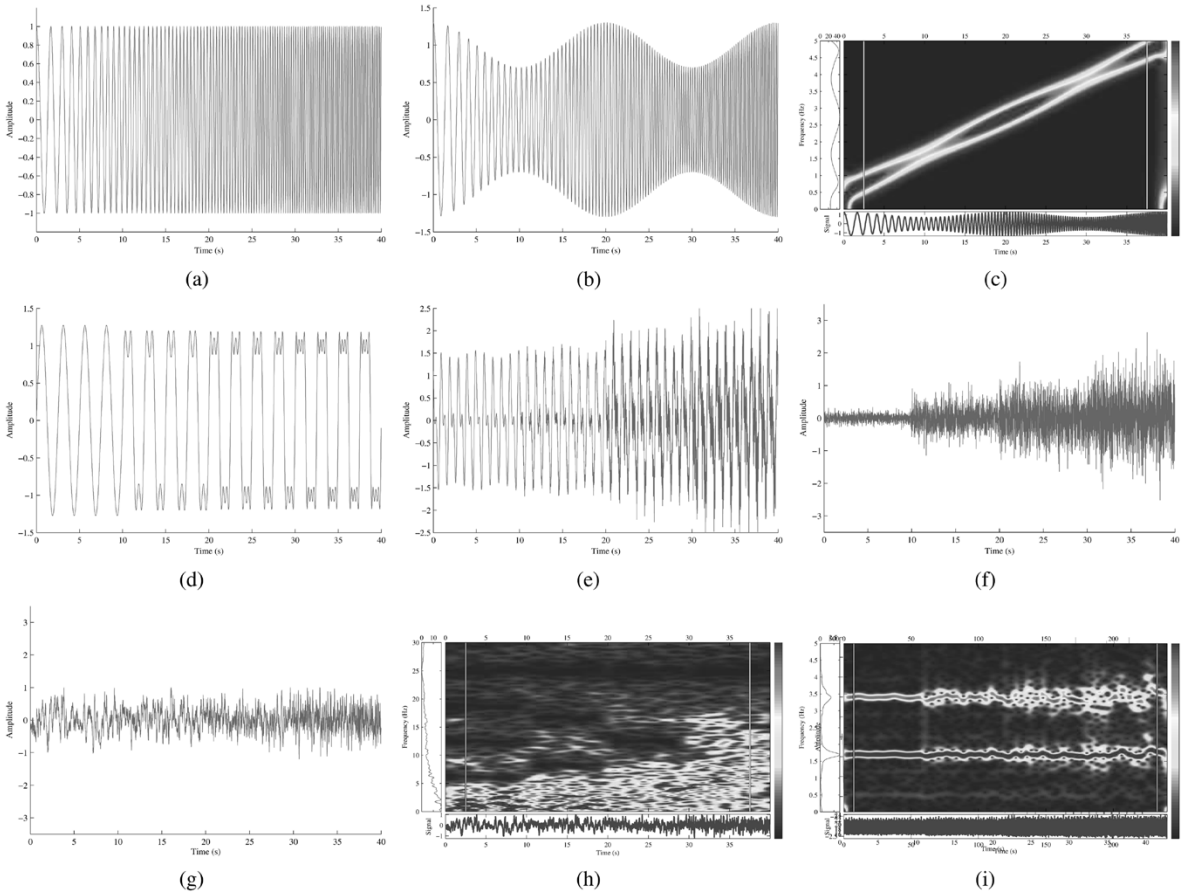

Fig. 2. Synthetic signals used in this study. (a) Chirp signal with constant amplitude ($f_1 = 0.5$, $f_2 = 5$ Hz). (b) Amplitude modulated chirp signal. (c) Spectrogram of the signal in (b). (d) Multi-tone signal used in Test 2. (e) Amplitude-modulated noisy signal with step increasing in noise power (Test 3). (f) White Gaussian Noise with step increases in noise power (Test 4). (g) Colored noise with step increases in noise bandwidth (Test 5). (h) Spectrogram of the signal shown in (g). (i) Spectrogram of the synthetic ICP signal with step increases in stochastic variability.

where $m_n(t)$, the normalized message signal, corresponds to respiration, and the carrier signal $\cos(2\pi f_c t)$ represents the pulsatile ABP or ICP components at the cardiac frequency. Since both ABP and ICP signals are composed of more than one harmonic and are not exactly periodic, the carrier signal $\cos(2\pi f_c t)$ does not provide an accurate model of ABP or ICP pulse pressure. However, we can model ABP and ICP as a modulation scheme where the carrier is not a pure sinusoid, but a periodic signal with more than one harmonic

$$p(t) = A_c[1 + ar_n(t)] \cdot \sum_{n=-N}^{N} C_n e^{j2\pi f_c n t} \tag{8}$$

where $r_n(t)$ is the normalize respiratory signal (i.e., $|r_n(t)| \leq 1$), and the carrier signal is a periodic signal with an arbitrary pulse morphology that has a Fourier series representation. The C_n coefficients can be determined from real ICP beats corresponding to different beat morphologies.

The pressure signal model $p(t)$ given in (8) can be simplified by considering only the first two harmonics (i.e., f_c and $2f_c$), since most of the power in real pressure signals is contained in the first two harmonics and the dc component. The simplified model is then

$$\begin{aligned} p(t) &= \mu_p + A_c[1 + ar_n(t)] \\ &\quad \cdot (\alpha \cos 2\pi f_c t + \beta \cos(4\pi f_c t + \theta)) \\ r(t) &= \sigma \cos 2\pi f_r t,\ r_n(t) = \cos 2\pi f_r t. \end{aligned} \tag{9}$$

According to this model, the normalized respiratory signal $r_n(t)$ modulates a carrier signal with a respiratory frequency f_r. The carrier signal is given by $c(t) = \alpha \cos 2\pi f_c t + \beta \cos(4\pi f_c t + \theta)$ and has a fundamental frequency of f_c (i.e., the cardiac frequency) and a second harmonic at twice the fundamental, α, β, and θ are chosen to generate a specific ICP morphology. For example, a typical ICP low pressure morphology can be synthesized by choosing $\alpha = 1$, $\beta = 0.5$ and $\theta = \pi/2$. The term $[1 + ar_n(t)]$ is always greater than zero.

The model for pressure signals given in (9) accounts for the AM effect that respiration has on pulse pressure, the constant cardiac component, and a reflected wave due to the changes in impedance in the arteries. However, it does not incorporate the effect of respiratory sinus arrhythmia (i.e., frequency modulation of the cardiac frequency with respiration).

Respiratory sinus arrhythmia was incorporated into the model by modeling f_c and f_r as as two correlated auto-regressive (AR) processes. Specifically, the cardiac and respiratory frequencies f_c and f_r were modeled as a sum of two components: a constant carrier frequency $\bar{f}$ an a stochastic frequency variation $\lambda(t)$

$$f_r(t) = \bar{f}_r + \lambda_r(t), \lambda_r(t) = -\sum_{k=1}^{P_1} a_k \lambda_r(t-k) + w(t)$$

$$f_c(t) = \bar{f}_c + \lambda_c(t), \lambda_c(t) = -\sum_{k=1}^{P2} b_k \lambda_c(t-k) + \eta(t)$$

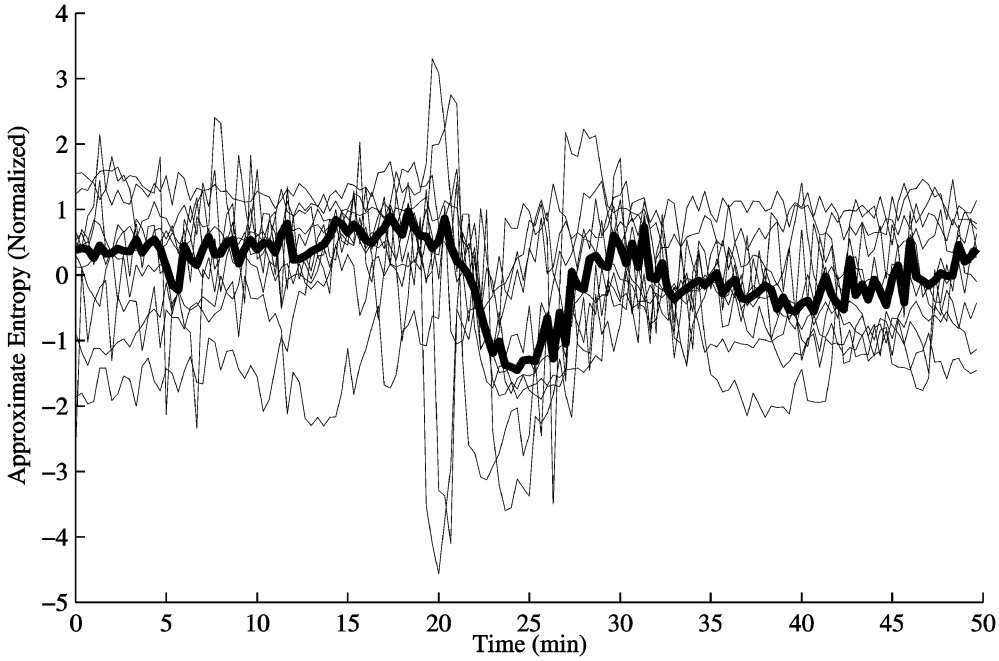

Fig. 3. ApEn (normalized) for each of ICH episode (light grey) and mean across all ICP spikes (dark). ApEn decreases as subjects progressed from a stable state of normal ICP (0–20 min) through the ICP spike and then returned toward normal with resolution of the sudden rise in ICP. This suggests that decreased complexity of ICP coincides periods of acute elevations in ICP in TBI.

$$+\sum_{k=0}^{Q} h_c(k)\lambda_r(t-k) \tag{10}$$

$$p(t)=\sum_{k=0}^{K-1} h(k,t) \times\left\{u_p+\left[1+a\sum_{l=1}^{K}\gamma_l e^{j2\pi\left(\sum \bar{f}_r+\lambda_r(t)\right)l(t-k)}\right] \cdot\sum_{n=1}^{N} C_n e^{j2\pi\left(\sum \bar{f}_c\lambda_c(t)\right)n(t-k)}+\kappa r(t-k)\right\} \tag{11}$$

where the cardiac $\lambda_c(t)$ and the respiratory $\lambda_r(t)$ stochastic frequency variations were modeled as two correlated auto-regressive (AR) processes.

7) ApEn Versus Respiratory and Heart Rate Variability: We generated a synthetic ICP signal with increasing stochastic variability in the frequency domain, by increasing the bandwidth of the AR processes that model the respiratory and cardiac frequencies.

We estimated the ApEn of the synthetic ICP signal using a moving window of 10 s with 90% overlap. Fig. 2(i) shows an spectrogram of the synthetic ICP signal.

IV. Results and Discussion

A. ApEn in ICP Signals During ICH

Fig. 3 shows a plot of the normalized ApEn for each of the 11 episodes and the median ApEn across all the episodes. From this figure we can see that
progressed from a stable state of normal ICP to a state of acutely elevated ICP. This indicates that decreased complexity of ICP coincides with episodes of ICH in TBI. The level of complexity begins to return to baseline levels within minutes as ICP drops below 20–25 mmHg. This decrease in complexity and irregularity in physiologic signals has been suggested to be directly related to severity of disease. Fig. 4 shows illustrative examples of the ApEn in six different subjects with TBI. Note how the ApEn decreases during periods of elevated ICP.

Table II shows the estimated mean ApEn during the stable, critical (ICH) and recovering regions for each of the 11 episodes, and the estimated standard errors corresponding to the ApEn means. The mean ApEn was lower during the ICH period than during the stable and recovering period in all the 11 episodes $(p < 0.01)$ (Table II). The population mean across all the 11 episodes during the stable, critical (ICH), and recovering regions were estimated to be 0.5158 ± 0.0089, 0.3887 ± 0.077, and 0.5096 ± 0.0158, respectively. Both the mean reduction in ApEn from the state of normal ICP (stable region) to the ICH region (-0.1271), and the increase in ApEn from the ICH region to the recovering region (0.1209) were determined to be statistically significant $(p < 0.01)$.

These results have three important implications. First, our results indicate that low ICP $AnEn$ coincides with episodes of intracranial hypertension (ICH). Decreased complexity during ICH has been hypothesized by several researchers, but this hypothesis has remained unproven, since none of the previous studies applied an established complexity measure such as ApEn to intracranial hypertension (ICH) episodes.

The fact that ICP ApEn decreases during periods of ICH demonstrates that there is information on the ICP beat morphology which correlates with patient condition. ApEn was applied to high-pass filtered ICP signals (i.e., without trend). Since the ApEn of the detrended ICP signal is inversely correlated with mean ICP, we can conclude that there is information contained on the ICP beat which correlates with patient condition. This finding provides the motivation for further research on ICP beat morphology analysis, since it establishes conclusively that there is information on the ICP beat.

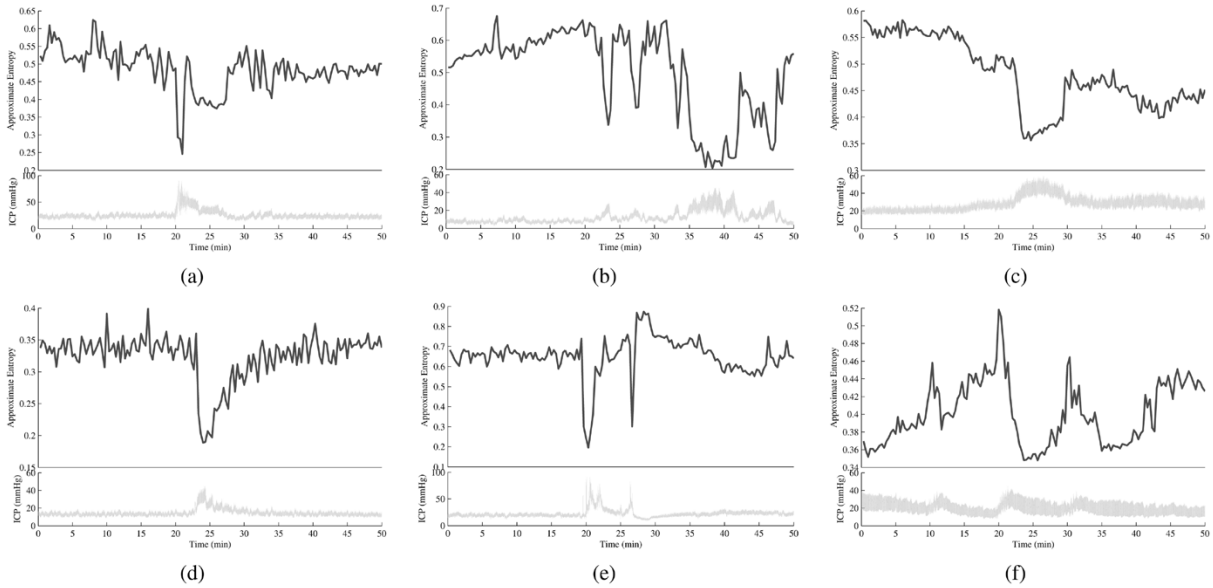

Fig. 4. Illustrative examples showing plots of the ApEn in six different subjects with TBI. Note how the ApEn decreases during periods of ICH.

TABLE II
MEAN ApEn OF THE ICP SIGNAL FOR STABLE (μ_s), CRITICAL (μ_c), AND RECOVERING REGIONS (μ_r) AND CORRESPONDING STANDARD ERRORS FOR STABLE (s_s), CRITICAL (s_c), AND RECOVERING REGIONS (s_r)

μ_s	μ_c	μ_r	s_s	s_c	s_r
0.643	0.262	0.759	0.0157	0.0209	0.0070
0.536	0.325	0.446	0.0060	0.0358	0.0153
0.548	0.387	0.539	0.0066	0.0032	0.0122
0.439	0.353	0.433	0.0037	0.0026	0.0095
0.499	0.336	0.377	0.0058	0.0069	0.0014
0.605	0.225	0.442	0.0142	0.0078	0.0094
0.507	0.363	0.466	0.0028	0.0024	0.0035
0.233	0.223	0.234	0.0006	0.0004	0.0005
0.329	0.225	0.325	0.0023	0.0015	0.0174
0.341	0.197	0.326	0.0060	0.0032	0.0078
0.315	0.185	0.277	0.0058	0.0023	0.0047

The third implication of our finding relates to noninvasive estimation of ICH (i.e., ICH detection without ICP monitoring). In general, decreased complexity in one physiologic signal often couples to other signals. Thus, by monitoring the ApEn of the ECG, ABP, SpO2 or EEG it may be possible to detect periods of ICH in the absence of the ICP signal.

B. ApEn *Interpretation*

Our simulation study was designed to enable researchers to interpret the ApEn metric in terms of classical signal processing concepts such as frequency, number of harmonics, frequency variability of harmonics, and signal bandwidth.

Previous work involving the application of ApEn has consisted on the application of this metric to a specific patient population or pathology, and identifying an ApEn change associated with a specific condition. However, the question of ApEn interpretability and its relationship to other signal parameters or metrics has not being previously addressed. Specifically, even though ApEn has been used extensively in biomedical research, none of the previous studies carried out a thorough simulation study on synthetic signals aimed at gaining a better understanding of ApEn itself.

Fig. 5 shows the results of tests performed to gain better understanding of ApEn and its interpretation in the context of biomedical signal analysis. Fig. 5(a) and (b) show the calculated ApEn for the signals shown in Fig. 2(a) and (b), respectively. From these two plots we conclude that ApEn increases as the frequency of a sinusoid increases, and that AM has an effect on ApEn (i.e., ApEn increases with the modulation index). Note that the ApEn values are slightly higher in the case of the amplitude modulated chirp signal than for the chirp signal with constant amplitude. This means that a signal with constant amplitude is slightly more regular or predictable than an amplitude modulated signal. Fig. 5(c) shows how the ApEn increases as the number of frequency components of a periodic signal increases. However, the ApEn values (from 0.05 to 0.07) are lower than ApEn values with the chirp signal, which indicates that periodic multi-tone signals are more regular and predictable (less complex) than chirp signals. In Fig. 5(d) and (e), we see that ApEn is sensitive to changes in noise power, increasing as the noise power increases. We notice that the increasing level is higher when there are signal and noise Fig. 5(d) than where there is only noise Fig. 5(e). Fig. 5(f) shows the relationship between ApEn and noise bandwidth, ApEn increases as the noise bandwidth increases. Fig. 5(g) demonstrates how the ApEn increases as the bandwidth of the AR processes modeling the respiratory and cardiac components increases. Thus, we conclude that increasing ApEn corresponds to a increasing system complexity [1].

Figs. 5(h) and (i) and 6 show the results of a Monte Carlo simulation aimed at determining the variance of the ApEn estimates. Fig. 5(i) shows the ApEn estimates for different realizations of the process shown in Fig. 5(f). Fig. 5(i) shows a histogram of the ApEn estimates on a white Gaussian noise process. Fig. 6 shows histograms of the ApEn calculated from 5000 realizations of a white Gaussian noise, white uniform noise, and colored noise. From the plot we see that the ApEn histograms corresponding to both white noise processes (white and nonwhite) have similar expected values and variance. However, ApEn is lower in the case of colored noise, and has more variance.

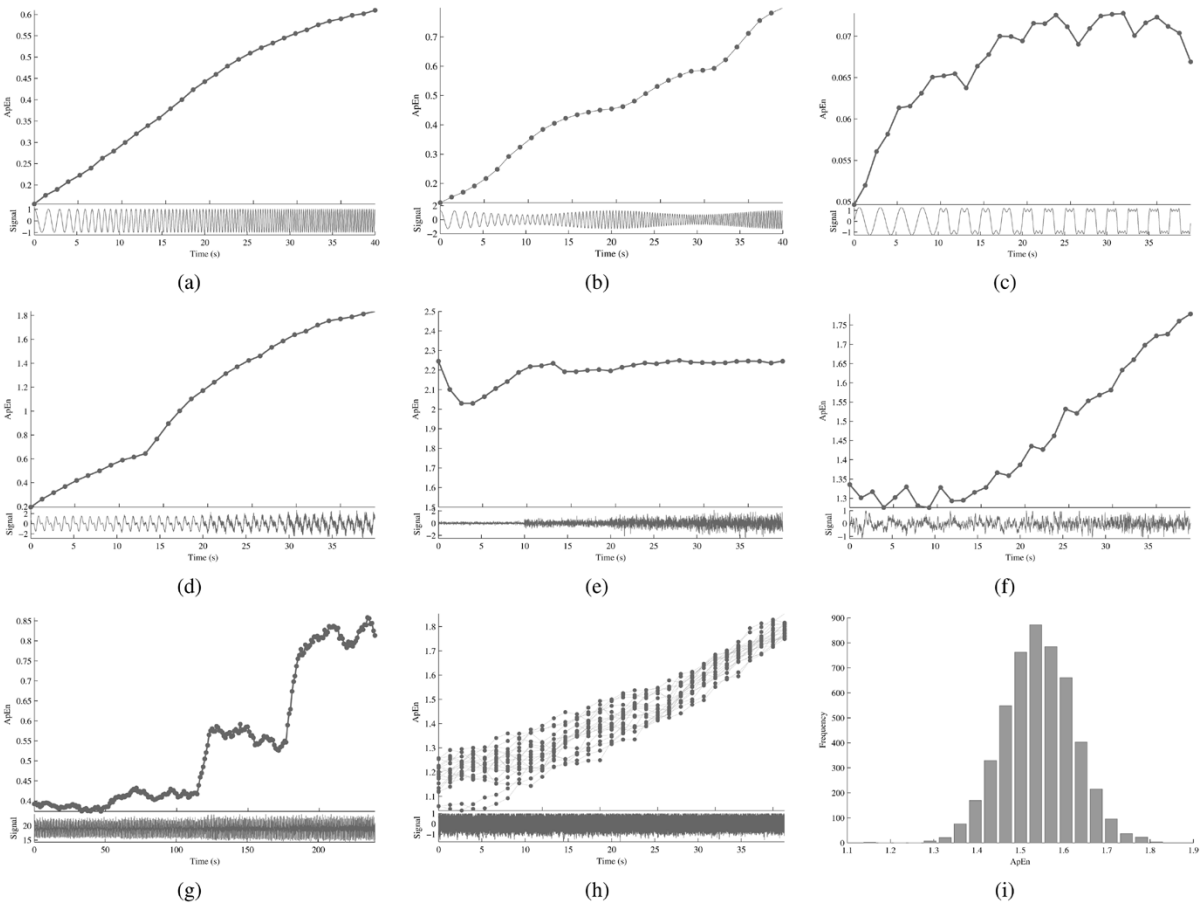

Fig. 5. Results of the tests performed to gain better understanding ApEn and its interpretation. (a) Relationship between ApEn and signal frequency, (b) ApEn and AM, (c) ApEn versus number of harmonics, (d) ApEn versus SNR, (e) ApEn versus noise power, (f) ApEn versus noise bandwidth, (f) ApEn versus stochastic variability of signal harmonics, (h-i) ApEn versus noise bandwidth variability.

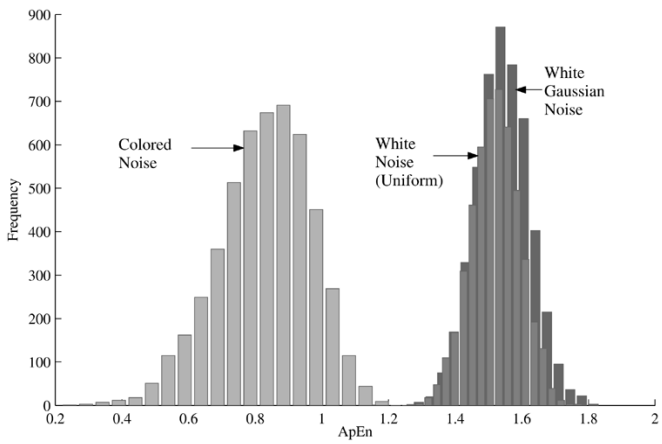

Fig. 6. Histograms of ApEn for white Gaussian noise, white uniform noise, and colored noise.

In the context of ICP and ICH, the test results enable us to interpret the changes ApEn during ICH episodes. Specifically, our results show that given a decreased on ApEn during a period of ICH, this can be due to 1) a reduction of signal harmonics (rounding effect), 2) increased variability of the cardiac component (interbeat variability), and/or 3) increased pulse amplitude [higher signal-to-noise ratio (SNR)]. This conclusion is a direct consequence of tests 2, 7, and (3–6), respectively. These findings are in accordance with the findings of the ICP research community for the past 25 years. The fact that ApEn correlates with the number of harmonics in periodic and quasi-periodic signals (as we have demonstrated with our simulation study) has important implications in the context of ICP analysis, since the number of harmonics of the signal directly relates to the morphology of the ICP beats (absence of higher harmonics results in a rounding of the ICP beat). Investigators have documented specific variations in the ICP beat morphology, which correspond to specific alterations in the cerebral vascular system, CSF circulation, and respiration. These morphology variations may be used to measure the progression of disease. For instance, Pornoy states that in patients who do not have a cerebral edema or expanding mass, the ICP beat shows an initial sharp rise and subsequent downward slope similar to the arterial pulse; but as the expanding mass or edema develops, the ICP pulse becomes more rounded. As the ICP pulse becomes more rounded the amplitude of the higher frequency sinusoidal components also decreases. Thus, based on these results, a decrease in ApEn during an ICP spike may be interpreted as a "decomplexification" or "loss of irregularity." This decomplexification may be associated with changes in time morphology or frequency metrics resulting in decreased time irregularity, frequency irregularity, or frequency bandwidth. This suggests that there is a natural progression of physiologic states from the time of injury, or onset of disease, through recovery or death. The physiologic state of the patient may shift rapidly from a compensated physiologic state to an uncompensated disease state as indicated by these results. Other investigators have described a number of metrics that change during ICP elevations.

Szewczykowski *et al.* described a "warning zone" in which the amplitude of ICP variations is strongly related to the mean ICP [32]. They hypothesized that this was caused by impaired compensating ability. Turner *et al.* observed that four patients who developed elevated ICP had increased variance over periods of 33 min prior to an ICP increase [33]. Several groups have found that an increase in the cardiac component[3] of the ICP signal precedes elevations [16], [34]. Czosnyka *et al.* observed a short spontaneous decrease in ABP at the beginning of plateau waves in eleven of sixteen cases [35].

A few investigators have also attempted time series prediction of the ICP signal [36]–[38]. These attempts employed wavelet decompositions to separate the signal into different frequency bands followed by neural networks to predict the wavelet coefficients, which were finally used to construct the predicted signal segments.

Our results suggest that the normal regulatory mechanisms that control cerebral blood flow, the cerebral autoregulation, are lost or impaired in severe TBI and completely fail during an acute elevation in ICP, resulting in decreased complexity and irregularity. Researchers have suggested that changes in system complexity at one level may reflect similar changes at more microscopic levels. Research to study biochemical and neurotransmitter changes and even molecular changes during severe TBI may show similar results of a decomplexification process.

V. Conclusion

We studied episodes of acute ICH in pediatric patients with severe TBI and found that the ApEn of ICP decreases during acute elevations. This suggests that the complex regulatory mechanisms that govern intracranial pressure are disrupted during acute rises in ICP. Additionally, we carried out a series of experiments where ApEn was used to analyze synthetic signals of different characteristics with the objective of gaining a better understanding of ApEn itself, specially with regards to its interpretability in the context of biomedical signal analysis and TBI. The results of our simulation study enable researchers to interpret the ApEn metric in terms of classical signal processing concepts such as frequency, number of harmonics, frequency variability of harmonics, and signal bandwidth. In summary, our simulation results show that 1) ApEn increases as the frequency and the number of harmonics of a sinusoidal signal increases, 2) ApEn is correlated with noise bandwidth, increasing as the noise bandwidth increases (ApEn is lower in the case of colored noise than for white noise), 3 typical values of ApEn for sinusoidal signals 0.001 to 0.007 $(m = 1, r = 0.25\sigma)$, and 4) the ApEn of biomedical signals increases as the variability of the cardiac component increases and decreases as the the pulse morphology becomes more rounded.

References

[1] S. Pincus, "Assessing serial irregularity and its implications for health," *Ann. NY Acad. Sci.*, vol. 954, pp. 245–267, 2001.

[2] A. Kolmogorov, "A new metric invariant of transient dynamical systems and automorphisms in lebesgue spaces," *Dokl. Akad. Nauk. SSSR*, vol. 119, pp. 861–864, 1958.

[3]The cardiac component of the ICP signal is defined as the frequency components that are near the heart rate.

[3] A. Wolf, J. Swift, H. Swinney, and J. Vastano, "Determining lyapunov exponents from a time-series," *Physica. D*, vol. 16, pp. 285–317, 1985.

[4] S. Pincus and A. Goldberger, "Physiological time series analysis: What does regularity quantify?," *Am. J. Physiol. (Heart Circ Physiol.)*, vol. 266, pp. H1643–H1656, 1994.

[5] S. Pincus, "Approximate entropy as a measure of system complexity," *Proc. Nat. Acad. Sci. USA*, vol. 88, pp. 2297–2301, 1991.

[6] J. Bruhn, H. Ropcke, B. Rehberg, T. Bouillon, and A. Hoeft, "Electroencephalogram approximate entropy correctly classifies the occurrence of burst suppression pattern as increasing anesthetic drug effect," *Anesthesiology*, vol. 93, pp. 981–985, 2000.

[7] M. Engoren, "Approximate entropy of respiratory rate and tidal volume during weaning from mechanical ventillation," *Crit. Care Med.*, vol. 26, pp. 1817–1823, 1998.

[8] S. Pincus, T. Cummings, and G. Haddad, "Heart rate control in normal and aborted SIDS infants," *Am. J. Physiol (Regulatory Integrative Comp. Physiol.)*, vol. 264, pp. R638–R646, 1993.

[9] L. Fleischer, S. Pincus, and S. Rosenbaum, "Approximate entropy of heart rate as a correlate of postoperative ventricular dysfunction," *Anesthesiology*, vol. 78, pp. 683–692, 1993.

[10] N. Radhakrishnan and B. Gangadhar, "Estimating regularity in epileptic seizure time series data," *IEEE Eng. Med. Biol. Mag.*, vol. 17, no. 3, pp. 89–94, May-Jun. 1998.

[11] I. Rezek and S. Roberts, "Stochastic complexity measures for physiological signal analysis," *IEEE Trans. Biomed. Eng.*, vol. 45, no. 9, pp. 1186–1191, Sep. 1998.

[12] X.-S. Zhang and R. Roy, "Derived fuzzy knowledge model for estimating the depth of anesthesia," *IEEE Trans. Biomed. Eng.*, vol. 48, no. 3, pp. 312–323, Mar. 2001.

[13] S. Pincus, "Older males secrete luteinizing hormone and testosterone more irregularly and joint more asynchronously, than younger males," *Proc. Nat. Acad. Sci. USA*, vol. 93, pp. 14 100–14 105, 1996.

[14] J. Veldhuis, M. Johnson, O. Veldhuis, M. Straume, and S. Pincus, "Impact of pulsatility on the ensemble orderliness (approximate entropy) of neurohormone secretion," *Am. J. Physiol. (Regulatory Integrative Comp. Physiol.)*, vol. 281, pp. R1975–R1985, 2001.

[15] P. Adelson and P. Kochanek, "Head injury in children," *J. Child Neurol.*, vol. 13, no. 1, pp. 2–15, 1998.

[16] D. Price, R. Dugdale, and J. Mason, "The control of ICP using three asynchronous closed loops," in *Intracranial Pressure IV*, Shulman, K. Marmarou, J. A. Miller, D. Becker, G. Hochwald, and M. Brock, Eds., 1980, pp. 395–399.

[17] T. G. Luerssen, "Intracranial pressure: Current status in monitoring and management," *Seminars Pediatric Neurol.*, vol. 4, no. 3, pp. 146–155, 1997.

[18] G. Y. Larsen and B. Goldstein, "Increased intracranial pressure," *Pediatrics Rev.*, vol. 20, pp. 234–239, 1999.

[19] S. Pincus, "Approximating markov chains," *Proc. Nat. Acad. Sci. USA*, vol. 89, pp. 4432–4436, 1992.

[20] S. Pincus and B. Singer, "Randomness and degrees of irregularity," *Proc. Nat. Acad. Sci. USA*, vol. 93, pp. 2083–2088, 1996.

[21] S. Pincus and D. Keefe, "Quantification of hormone pulsatility via an approximate entropy algorithm," *Am. J. Physiol. (Endocrinol Metab)*, vol. 262, pp. E741–E754, 1992.

[22] Y. Fusheng, H. Bo, and T. Qingyu, "Approximate entropy and its application in biosignal analysis," in *Nonlinear Biomedical Signal Processing Volume II: Dynamic Analysis and Modeling*. ser. Biomedical Engineering, M. Akay, Ed. Piscataway, NJ: IEEE Press, 2001.

[23] D. Lake, J. Richman, M. Griffin, and J. Moorman, "Sample entropy analysis of neonatal heart rate variability," *Am. J. Physiol. (Regulatory Integrative Comp. Physiol.)*, vol. 283, pp. R789–R797, 2002.

[24] D. Kaplan, M. Furman, S. Pincus, S. Ryan, L. Lipsitz, and A. Goldberger, "Aging and the complexity of cardiovascular dynamics," *Biophys. J.*, vol. 59, pp. 945–949, 1991.

[25] B. Goldstein, J. McNames, B. McDonald, M. Ellenby, S. Lai, Z. Sun, D. Krieger, and R. Sclabassi, "A physiologic data acquisition system and database for the study of disease dynamics in the intensive care unit," *Crit. Care Med.*, vol. 31, pp. 433–411, 2003.

[26] P. Andelson, S. Bratton, R. Chesnut, H. du Cordray, B. Goldstein, P. Kochanek, H. Miller, M. Partington, N. Selden, C. Warden, and D. Wright, "Guidelines for the acute medical management of traumatic brain injury in infacts, children and adolescents," *Crit. Care Med.*, no. 31, pp. S417–S490, 2003.

[27] E. G. Caiani, M. Turiel, S. Muzzupappa, A. Porta, L. P. Colombo, and G. Baselli, "Noninvasive quantification of respiratory modulation on left ventricular size and stroke volume," *Physiolog. Meas.*, vol. 23, pp. 567–580, 2002.

[28] E. G. Caiani, M. Turiel, S. Muzzupappa, A. Porta, G. Baselli, S. Cerutti, and A. Malliani, "Evaluation of respiratory influences on left ventricular function parameters extracted from echocardiographic acoustic quantification," *Physiolog. Meas.*, vol. 21, pp. 175–186, 2000.

[29] F. Michard, D. Boussat, D. Chemla, and N. Anguel, "Relation between respiratory changes in arterial pulse pressure and fluid responsiveness in septic patients with acute circulatory failure," *Am. J. Respir. Crit. Care Med.*, vol. 162, pp. 134–138, 2000.
[30] F. Michard, D. Chemla, and C. Richard, "Clinical use of respiratory changes in arterial pulse pressure to monitor the hemodynamic effects of PEEP," *Am. J. Respir Crit. Care Med.*, vol. 159, pp. 935–939, 1998.
[31] L. J. Brada, W. H. Cooke, J. Hoag, A. A. Crossman, T. A. Kuusela, K. U. Tahvanainen, and D. L. Eckberg, "Respiratory modulation of human autonomic rhythms," *Am. J. Physiol Heart Circ. Physiol.*, vol. 280, pp. H2674–H2688, 2001.
[32] J. Szewczykowski, P. Dytko, A. Kunicki, J. Korsak-Sliwka, S. Sliwka, J. Dziduszko, and B. Augustyniak, "Determination of critical ICP levels in neurosurgical patients: A statistical approach," *Intracranial Pressure II*, pp. 392–393, 1975.
[33] J. Turner, D. McDowall, R. Gibson, and H. Khaili, "Computer analysis of intracranial pressure measurements: Clinical value and nursing response," in *Intracranial Pressure III*, J. Beks, D. Bosch, and M. Brock, Eds., 1976, pp. 283–287.
[34] H. D. Portnoy and M. Chopp, "Cerebrospinal fluid pulse wave form analysis during hypercapnia and hypoxia," *Neurosurgery*, vol. 9, no. 1, pp. 14–27, 1981.
[35] M. Czosnyka, P. Smielewski, S. Piechnik, E. A. Schmidt, P. G. Al-Rawi, P. J. Kirkpatrick, and J. D. Pickard, "Hemodynamic characterization of intracranial pressure plateau waves in head-injured patients," *J. Neurosurg.*, vol. 91, no. 1, pp. 11–19, 1999.
[36] F.-C. Tsui, C.-C. Li, M. Sun, and R. J. Sclabassi, "Multiresolution dynamic predictor based on neural networks," *SPIE Proc.*, vol. 2762, pp. 220–230, 1996.
[37] ——, "Acquiring, modeling, and predicting intracranial pressure in the intensive care unit," *Biomed. Eng. Applicat. Basis Commun.*, vol. 8, no. 6, pp. 566–578, 1996.
[38] M. Swiercz, Z. Mariak, J. Krejza, J. Lewko, and P. Szydlik, "Intracranial pressure processing with artificial neural networks: Prediction of ICP trends," *Acta Neurochir (Wien)*, vol. 142, no. 4, pp. 401–406, 2000.

Roberto Hornero (M'04) was born in Plasencia, Spain, in 1972. He received the engineer degree in telecommunications engineering and the Ph.D. degree from University of Valladolid, Valladolid, Spain, in 1995 and 1998, respectively.

He is currently an Associate Professor (Profesor Titular) in the Signal Theory and Communications Department at University of Valladolid. His main research interest is nonlinear analysis of biomedical signals. He founded the Biomedical Engineering Group in 2004. The research interests of this group include nonlinear dynamics, chaotic theory, and wavelet transform with applications in biomedical signal and image processing. He is a member of the Spanish Biomedical Engineering Society (SEIB).

Mateo Aboy (M'98) received the double B.S. degree (*magna cum laude*) in electrical engineering and physics from Portland State University (PSU), Portland, OR, in 2002. In 2004, he received the M.S. degree (*summa cum laude*) in electrical and computer engineering from PSU and the M.Phil (DEA) degree from the University of Vigo (ETSIT-Vigo), Vigo, Spain, where he is working towards the Ph.D. degree in the Signal Theory and Communications Department.

Since September 2000, he have been a research member of the Biomedical Signal Processing Laboratory (PSU). He has been with the Electronics Engineering Technology Department at Oregon Institute of Technology, Portland, since 2005. His primary research interest is statistical signal processing.

Mr. Aboy is a lifetime honorary member of the Golden-Key Honor Society, a past Chapter President of HKN (International Electrical Engineering Honor Society), and past Corresponding Secretary of TBP (National Engineering Honor Society).

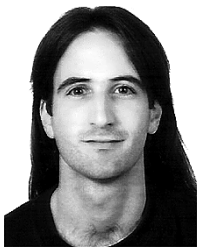

Daniel Abásolo (M'04) was born in Valladolid, Spain, in 1976. He received the engineer degree in telecommunications engineering from the University of Valladolid, in 2001.

Currently, he is a Lecturer in the Signal Theory and Communications Department at University of Valladolid. His main research interest is nonlinear biomedical signal processing. He is a member of the Biomedical Engineering Group and of the Spanish Biomedical Engineering Society (SEIB).

James McNames (M'99–SM'03) received the B.S. degree in electrical engineering from California Polytechnic State University, San Luis Obispo, in 1992. He received M.S. and Ph.D. degrees in electrical engineering from Stanford University, Stanford, CA, in 1995 and 1999, respectively.

He has been with the Electrical and Computer Engineering Department at Portland State University, Portland, OR since 1999, where he is currently an Associate Professor. He has published over 90 journal and conference papers. His primary research interest is statistical signal processing with biomedical applications.

He founded the Biomedical Signal Processing (BSP) Laboratory (bsp.pdx.edu) in fall 2000. The mission of the BSP Laboratory is to advance the art and science of extracting clinically significant information from physiologic signals. Members of the BSP Laboratory primarily focus on clinical projects in which the extracted information can help physicians make better critical decisions and improve patient outcome.

Brahm Goldstein (A'99) received the B.S. degree in biological science from Northwestern University, Evanston, IL, in 1977 and the M.D. degree from the State University of New York (SUNY) Upstate Medical Center at Syracuse in 1981. His clinical training included residency in pediatrics at the University of California at Los Angeles (UCLA) Medical Center and fellowships in pediatric cardiology and pediatric critical care medicine at Children's Hospital and Massachusetts General Hospital, Boston, respectively.

After serving as a faculty member at the Harvard Medical School, Cambridge, MA, and at the University of Rochester School of Medicine and Dentistry, Rochester, MN, he joined the Oregon Health & Science University, Portland, where he now is Professor of Pediatrics and Director of the Pediatric Clinical Research Office. His research interests include the study of heart rate variability and the acquisition and analysis of biomedical signals in critical illness and injury (brain injury and septic shock in particular). He formed the Complex Systems Laboratory (www.ohsuhealth/dch/complex) in 1998 to study complex disease states in critically ill and injured children.

Dr. Goldstein is a diplomate of the American Board of Pediatrics and its subboard pediatric critical care medicine.